Essential Readings in Light Metals: Aluminum Reduction Technology.
Edited by Geoff Bearne, Marc Dupuis and Gary Tarcy.

DESIGN CONSIDERATIONS FOR SELECTING THE NUMBER OF POINT FEEDERS IN MODERN REDUCTION CELLS

M. L. Walker[a], J. M. Purdie[b], N.S. Wai-Poi[b], B.J. Welch[a], J.J.J. Chen[a]

(a) Chemical and Materials Engineering Department
University of Auckland, New Zealand.

(b) Comalco Research Centre, 15 Edgars Road
Thomastown, Melbourne, Vic. 3074, Australia

ABSTRACT

Point feeding systems are now installed in most modern reduction cells in preference to bar breakers. The main reason for this choice is that point feeders allow improved alumina dissolution. However complete alumina dissolution is not an explicit design criterion for selecting the size of the alumina dump or the number of feeders required.

In this paper, three performance criteria for determining the number of point feeders required in a cell are investigated. These are: acceptable alumina dissolution, satisfactory mixing to avoid concentration gradients and a satisfactory rate of alumina concentration increase after anode effect. Using a combination of laboratory data and measurements from industrial cells, it is shown that the alumina dissolution requirement is likely to be the most difficult to satisfy. Complete alumina dissolution upon addition is unlikely to be achieved with the point feeder designs installed in most modern cells.

1. INTRODUCTION

In older cell designs, alumina feeding is a relatively infrequent operation. Sidebreak feeders typically feed at two to four hourly intervals, and centre bar breakers at intervals of around one hour. The alumina fed is not dissolved immediately upon addition, because of heat and mass transfer constraints [1-3]. Agglomerates of frozen electrolyte and alumina, known as 'sludge' or 'muck', sink to the bottom of the cell and are gradually redissolved over the period leading up to the next feed.

The presence of large reserves of sludge limits cell performance. Alumina concentration in the electrolyte depends on the rate at which sludge redissolves, and is therefore not well controlled. Large reserves of sludge lead to operating problems, such as anode spikes, burn-offs and voltage instability. Regular anode effects have historically been included in control strategies to control sludge levels.

Modern cell technologies aim to improve feed control and to operate with less sludge present, and for this reason point feeding systems are installed. Small amounts of alumina are fed at frequent intervals, to minimise both the thermal effect of the alumina addition and the tendency to form sludge.

Although improved alumina dissolution is the main justification for the increased capital cost of a point feeder design, when a new cell design or retrofit proposal is developed the number of feeders and size of feeds appears to be determined empirically. It is difficult to confirm that alumina added from a point feeder is completely dissolved, and this is probably why good dissolution performance is not an explicit design criterion.

A typical cell has 3 to 5 feeders, each delivering a charge of 1 to 5 kg. The number of feeders depends to some extent on the size of the cell, and there is often approximately one feeder for every 50 kA of cell current, although industry practice varies. For example, the Pechiney AP18 and AP30 designs are understood each to have 4 feeders, although one operates at 180kA and one at 300 kA. Other factors such as hopper utilisation and cell operability in the event of failure of one feeder are also considered.

In this paper three performance-related criteria for determining the number of point feeders required in a cell are investigated - alumina dissolution, concentration gradients and concentration rise after anode effect.

Measurements made in a physical model allow the mass of electrolyte in the feeder mixing zone, and the maximum point feed addition which can be dissolved completely, to be estimated for the cell design simulated. The results have been compared with tracer measurements in an industrial cell. The rate at which continuously fed alumina can be dissolved upon addition has also been measured in the laboratory. From these results, the maximum rate of continuous alumina feeding for complete dissolution upon addition has been predicted.

Industrial measurements of mixing rate, using a tracer technique, have been reported previously[4]. A simple mathematical model, which fits these measurements, is presented. The rate of concentration rise following a feed, and steady state concentration gradients during point feeding, are predicted.

2. ESTIMATING THE SIZE OF THE FEED MIXING ZONE.

A full scale, kinematically similar three dimensional physical model of a Hall-Heroult cell has been used to study the mixing characteristics of the region close to a point addition site. A coloured solution was initially used as the tracer. Subsequent comparison with plant measurements showed that mixing of crushed ice better modelled the behaviour of a tracer in the electrolyte of an operating cell, and therefore, it is assumed, the distribution of alumina. The ice addition technique was then used to estimate the size of the well mixed zone around a point feeder, and to predict the effects of feeder location and anode tilt on the distribution rate of alumina, in an operating cell.

2.1 Solution Tracer Experiments in Model

The model comprised two full scale anodes installed in a glass walled tank, with one side shaped to represent the side ledge (as in Figure 1). Water was used to model the electrolyte phase, and anodic gas formation was simulated by forcing air through porous polyethylene sheets on the anode base. It was assumed that the vertical glass wall of the tank, in the centre channel, operated as a mirror plane of the flow field. The metal phase was not modelled and was assumed to be a solid, horizontal interface. Different cell geometries were simulated by varying the parameters electrolyte depth, centre and side channel width and anode slope.

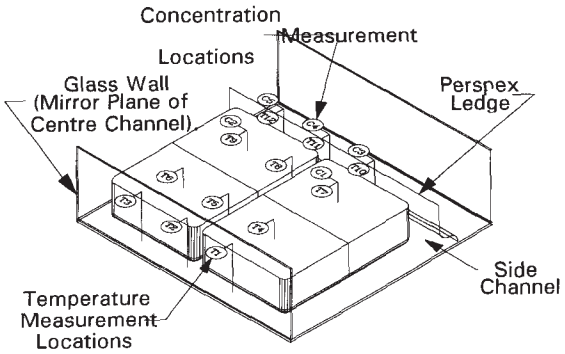

Figure 1: Physical Model

In the first set of experiments, blue indicator dye was added to the model to simulate an alumina addition. The concentration of dye was measured at 5 locations around the cell at 10 s intervals, by drawing a continuous stream of water/dye solution (representing electrolyte) through continuous flow cells inside a computer controlled UV/VIS spectrophotometer. The dye flow patterns were recorded by cameras beneath the model tank.

The results indicated that mixing throughout the region surrounding the two anodes would occur very rapidly. For a point addition in the centre channel, complete concentration equilibrium within the model was achieved after only 300 s.

2.2 Tracer Dispersion Trials in Industrial Cells

These results were not consistent with mixing times reported previously for tracer experiments in industrial cells[4], where equilibrium concentration throughout the cell was achieved only after about 30 minutes. Further industrial experiments were performed to study mixing around anodes near the addition point in more detail. A 1kg sample of tracer was added to the centre channel of the cell, and electrolyte samples were taken at 15 s intervals.

The mixing curves obtained (Figure 2) were consistent with the previously reported mixing times of the order of 30 minutes. (Referring to the water model geometry in Figure 1, the addition was at an equivalent position to T2, and samples were taken at positions equivalent to T11, on both upstream and downstream sides of the cell, and T10 or T12.) The significantly longer mixing times compared with the water model indicated that factors important to distribution in the industrial cell had not been modelled in the solution tracer experiments.

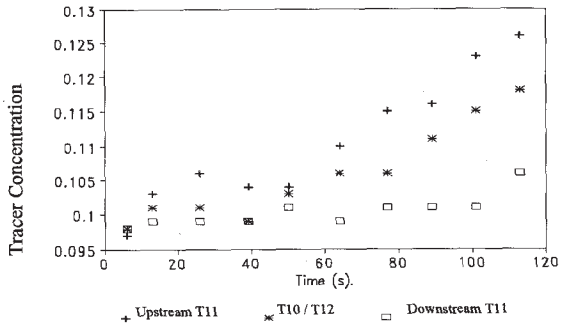

Figure 2: Tracer Addition to Operating Cell

The formation of agglomerates, as reported in alumina dissolution studies[5,6,11-13], is likely to be one factor retarding tracer, and alumina, distribution. These agglomerates, some of which float as 'rafts' on the surface of the electrolyte, result from the sudden freezing of electrolyte onto the cold alumina. Non-buoyant agglomerates are entrained in the turbulent centre-channel flow and are distributed throughout the mixing zone, whilst floating alumina agglomerates remain on the electrolyte surface, transported only by surface currents.

2.3 Particulate Tracer Experiments in the Model

To model the remelting of 'rafts' in the centre channel, additions of 1 kg of packed crushed ice were made to the water model. The break-up and melting of the ice 'rafts' and the transport of small non-buoyant ice particles was observed visually, while temperatures throughout the model cell were monitored with thermocouples connected to a data acquisition system.

Figure 3 illustrates the temperature response, at the positions shown in Figure 1, following a single ice addition in the centre channel of the model cell (addition made at position T2, anodes sloped towards the centre channel). To display the traces clearly in one Figure, the origins of the temperature records have been shifted, with thermocouple 4 being moved 4° C and so on. The temperature transients recorded in the side channel region appear to be on a similar time scale and have a similar shape to the concentration transients measured in the tracer addition experiments (Figure 2). The ice rafts typically melted after approximately 1 minute, giving them a similar 'life' to alumina rafts observed in laboratory studies[5,6] , which disappear after about 1 minute. These observations suggest that ice addition is a reasonable model for the dynamics of tracer addition, and alumina addition, in the industrial cell.

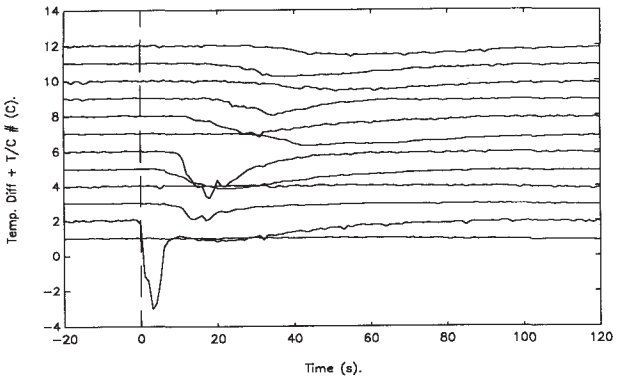

Figure 3: Temperature Response Following Centre Channel Ice Addition

Compared with the dye addition experiments, the ice addition experiments showed similar directional flow characteristics but the rate of mixing was considerably slower for the ice additions. The general flow pattern observed in the centre channel region, for anodes sloped towards the centre channel, is illustrated in Figure 4. Once dissolved, the tracer moves into the slot, under an anode and back into an adjacent mixing volume. This recirculation further delays distribution of dissolved material from the centre channel to other regions of the cell, and contributes to the slow mixing observed in industrial cells.

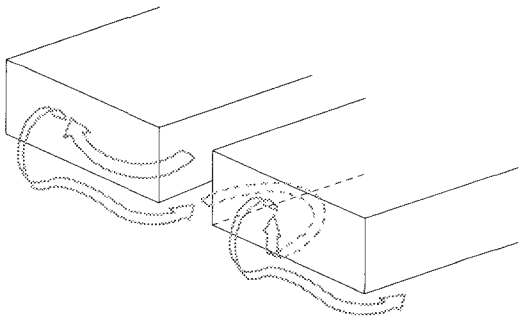

Figure 4: Centre Channel Flow Pattern

The flow patterns observed differ somewhat from previous numerical modelling predictions, where flow from the centre channel into the slots was less apparent. The numerical model considered a flat anode, (never achieved in practice except on a new anode) whereas the water model anodes were sloped at 2° towards the centre channel. Small differences in anode slope (for example at different anode positions due to the shape of the metal pad), can clearly have a significant effect on electrolyte flow, and may contribute to process variation in the cell.

2.4 Model Cell Studies - Size of The Mixing Zone

The ice rafts formed by addition of ice to centre channel locations T1 and T3 (see Figure 1) drifted in the centre channel along the width of the anode, due to surface currents. The rafts rarely moved through the two impinging fluid jets issuing from the slots on either side of the centre channel. The temperature of the electrolyte phase in the centre channel (T3) was largely unaffected by an ice addition at position T1, supporting the conclusion that there is little movement along the centre channel past a slot.

Ice particles stripped from the agglomerate were turbulently mixed within the volume beneath this surface, and did not readily move out of this region either along the centre channel or into the inter-anode slot until dissolved.

This leads to the conclusion that mixing and dissolution of point-fed material is limited to the centre-channel region, along the width of one anode.

2.5 Prediction of Feed Mixing Zone Size in Industrial Cells

Assuming that the ice-water system accurately models the mixing of alumina in a cell following a point feed addition, the electrolyte mass available in the feed mixing volume has been estimated as 80 kg for the cell design modelled. The maximum alumina addition to which sufficient enthalpy for preheat and complete dissolution can be supplied from this volume, without the electrolyte being cooled below its liquidus temperature, is then approximately 0.6 kg. The calculations assume an anode width along the cell of 800 mm, centre channel width 250 mm, electrolyte depth 200 mm, and superheat 10°C. Alumina dissolution enthalpy has been taken as 1500 kJ/kg, assuming 4 % initial alumina concentration[7], and specific heat over the temperature range has been taken as 1200 J/kg[8] and electrolyte (cryolite) heat capacity as 1880 J/kg[8].

If the cell operates at 160 kA, the alumina requirement is approximately 1.6 kg/minute (at 95 % current efficiency). With three point feeders installed in the cell and a dumpweight of 0.6 kg, each feeder would be required to operate every 70 seconds. Feeder operation at two minute intervals is thought to be more typical of industry practice, and problems such as buildup of frozen electrolyte on point breakers can occur if the time between breaker operation is insufficient for the breakers to cool. At this operating frequency five point feeders would be required. For comparison, with current industry design practices either three or four feeders would be installed in a cell of this size.

The temperature transients in Figure 3 show that some mixing can occur with the fluid mass in the ACD region, potentially providing additional heat to the mixing zone, although the undissolved particles generally remain in the centre channel. The above calculation therefore underestimates the heat available at the assumed superheat, and represents a 'worst case' scenario. Although exact quantitative predictions of the maximum feed mass cannot be made, the results clearly show that there is limited movement of electrolyte between side and centre channel and along the centre channel, and that the mass of electrolyte into which alumina is dissolved is small relative to the total mass in the cell.

Addition of an alumina mass large enough to cool the mixing zone to its liquidus temperature will retard heat exchange to, and dissolution of, the alumina agglomerate. Under these conditions it is thought likely that dissolution will be delayed to the point where sludge formation can occur.

2.6 Effect of Feeder Location

When ice was added near the inter-anode slot, mixing was improved. The fluid jet issuing from the slot split the ice raft into smaller agglomerates, which moved into the centre channel regions on either side of the slot. By locating a feeder in this position, the size of the effective mixing zone can be doubled, and the number of feeders required to achieve good dissolution is halved.

3. DISSOLUTION RATE FOR CONTINUOUSLY FED ALUMINA

In this set of experiments, the dissolution rate of continuously fed alumina in molten cryolite was measured under different heat and mass transfer conditions, to determine the maximum dissolution rate at which alumina can be added without risk of sludge formation.

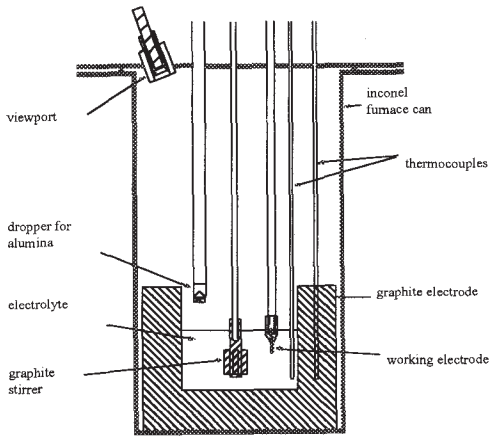

Figure 5: Experimental Apparatus for Dissolution Measurements

3.1 Experimental Technique

The in situ electroanalytic technique used to measure alumina concentration was based on a modified form of linear sweep voltammetry. The experimental apparatus used has been described previously[5,6,11] and is shown in Figure 5. The electrolyte had a bath ratio of 1.18. The graphite stirrer used enabled velocities of up to 30 cm/s, of similar magnitude to values between 15 and 35 cm/s reported in industrial cells[9,10], to be achieved.

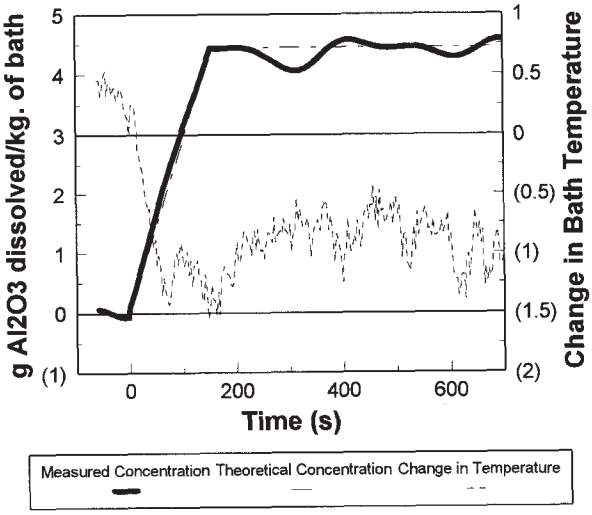

Figure 6: Fast Dissolution

3.2 Observations of Dissolution Behaviour

Two types of dissolution were observed, a 'fast' dissolution and a slower 'two stage' process. A typical 'fast' result is illustrated in Figure 6. The experimentally measured rate of alumina concentration increase and the alumina feed rate are in good agreement. This indicates that the alumina powder is dispersing and dissolving rapidly on addition to the electrolyte, and that alumina/frozen electrolyte agglomerates are not being formed.

A 'two stage' dissolution is shown in Figure 7. Similar behaviour has been reported previously[2,11,12] and is characteristic of alumina aggregation[13]. In the first stage of the dissolution, in the period 0 to 190 seconds, the dissolution rate is constant and is appreciably lower than the feed rate. The alumina which is not dissolving upon addition forms agglomerates or rafts upon the electrolyte surface, as discussed in Section 2. Dissolution of these rafts continues after alumina addition has ceased, at a slower rate.

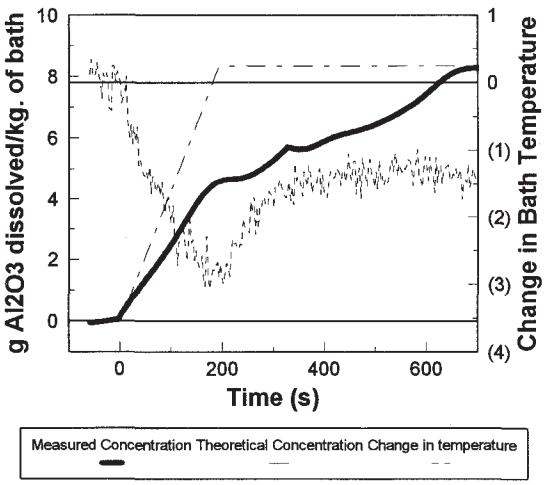

Figure 7: Two stage alumina dissolution

The addition rate at which two-stage dissolution is first observed gives the maximum addition rate for immediate dissolution, under the experimental conditions. When alumina is dissolving immediately, there is no possibility of sludge being formed, and the measured rate therefore represents the maximum addition rate at which there is no risk of sludge formation. In the cell, once rafts begin to form, some of the agglomerated material may later sink beneath the metal pad to form sludge. Alternatively, the rafts may break up in the turbulent flow and dissolve completely, as observed in the water model experiments.

3.3 Maximum Addition Rate for Good Dissolution

Table 1 presents the results from several dissolution experiments under different heat and mass transfer conditions. Dissolution rates of between 1.4 and 3.0 g/min per kg of electrolyte were achieved, the higher rates being achieved at higher superheats and stirring rates and lower alumina concentrations. For the cell design discussed in Section 2, the addition rate for immediate alumina dissolution is at most only 0.25 kg/minute (assuming a dissolution rate of 3.0 g/min.kg is achieved, and the geometry in Section 2.5). If the cell were operating at an amperage of 160 kA, seven feeders would be required to supply alumina at the consumption rate of around 1.6 kg/minute.

From these results, a large number of alumina feeders would required to avoid potential sludge formation, even if feeding were continuous.

Plant trials are required to validate these results, however, as mass transfer in the industrial situation may not be accurately modelled in the laboratory, and results show that the maximum dissolution rate achieved is highly dependent upon mass transfer. It is also important to determine under what conditions the alumina rafts dissolve satisfactorily without forming sludge.

4. MATHEMATICAL MODELLING OF THE INDUSTRIAL SITUATION

A tracer technique for measuring mixing times in industrial cells has been described previously[4]. This technique was used on a cell of the design described in Section 2. Semi-empirical models were developed, and fitted to the data, to predict the rate of increase of alumina concentration after depletion to anode effect and the extent of concentration gradients set up in the cell.

4.1 Experimental Measurements

Raw and averaged data from two tracer additions at the tap end of the cell is presented in Figure 8. The duct end average is the average of two experiments. As the sidechannel sample locations were different in the two experiments, the average sidechannel concentration represents the average of measurements in the centre of the upstream and downstream sidechannels in one experiment.

Even distribution of the tracer around the cell took 30 to 45 minutes, which is a similar result to the 30 to 40 minute mixing time reported previously on a cell of a different design[2]. Asymmetric flow patterns were again observed, with tracer added at the tap end being transported to the downstream side more rapidly than upstream on this cell.

Table 1: Initial Operating Parameters and Dissolution Results

Trial	Bath Ratio	Initial Superheat (°C)	Stirrer Speed (RPM)*	Initial Al_2O_3 Concentration (wt%)	Feed Rate (g/min.kg bath)	Dissolution Rate (g/min.kg bath)
1	1.18	8	200	0.7	2.6	1.4
2		9	200	0.7	2.1	1.4
3		9	300	0.7	1.6	1.6
4		14	300	0.7/1.1	3.0/2.1	3.0/2.1
5		7	300	0.7/1.1	3.3/3.7	2.6/2.0

* Note: 300 RPM gives an electrolyte velocity of approximately 30 cm/s

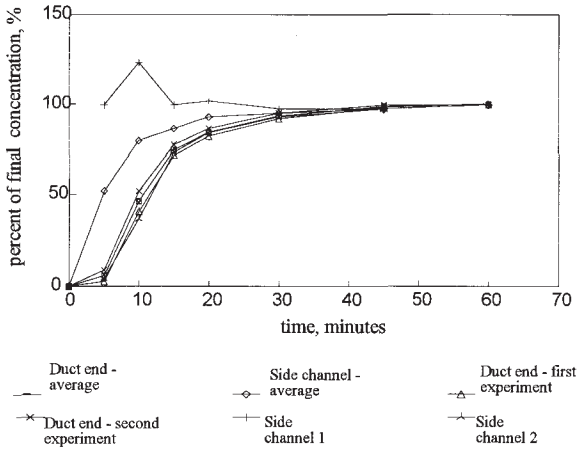

Figure 8: Average mixing times in cell

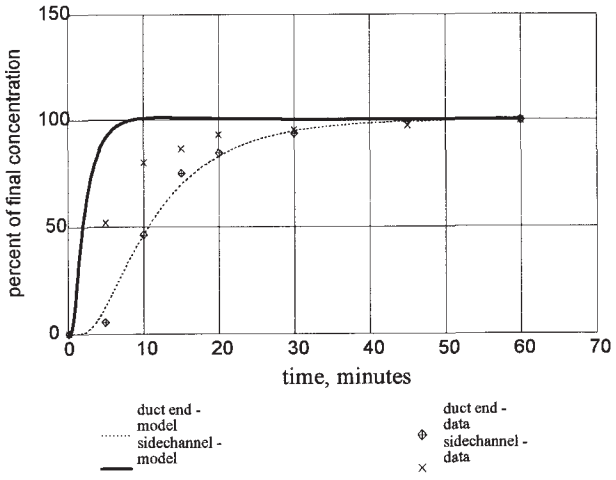

Figure 9: Model fit to data with D = 0.018 m^2/s

4.2 Development of Model

To estimate the time taken for alumina to be distributed from a feed location around the cell, a semi-empirical model has been developed, in which mixing is assumed to be governed by an 'effective diffusivity' parameter. The model can be applied to cells for which experimental mixing rate data is available. The two-dimensional time-dependent diffusion equations are solved with zero-flux boundary conditions, using finite difference methods. The reduced height of the flow field beneath anodes is accounted for by considering each node of the finite difference grid as a control volume, with the flux between adjacent volumes proportional to the height of their interface.

The implicit assumptions here are that directional flow occurs on a scale much smaller than the dimensions of the cell, so that electrolyte flow is effectively non-directional. Mixing rate can then be characterised by an 'effective diffusivity parameter' which depends upon electrolyte turbulence. The value of this parameter is chosen to best fit the concentration transient at the opposite end of the cell from the addition point, so to represent the mixing rate along the cell, which is important for determining how may feeders are needed in the cell.

This model has been used to predict mixing rates for the cell design previously described. In Figure 9, the concentration transients predicted using different values of the effective diffusivity, D_{eff}, are compared with data. The best fit at the opposite end of the cell was for a value of 0.018 m^2s^{-1} and the shapes of measured and predicted transients are similar. A lower value would have given a better fit to the sidechannel transient. However as the two sidechannel transients are markedly different, because the flow is asymmetric, the value of fitting the model data to the average sidechannel transient is questionable.

4.3 Increasing Alumina Concentration after Anode Effect

The definition of a satisfactory concentration increase after anode effect is to some extent arbitrary. For this study, alumina distribution was defined as satisfactory when, following an addition, the concentration throughout the cell reached fifty percent of its final value within one minute. This was based on the assumptions that the control strategy would aim to increase net alumina concentration by one to two percent and to extinguish an anode effect within one minute, and that an increase in alumina concentration throughout the cell of half this size would be sufficient for the anode effect to be terminated[14,15]. Alumina dissolution at anode effect was assumed to be instantaneous.

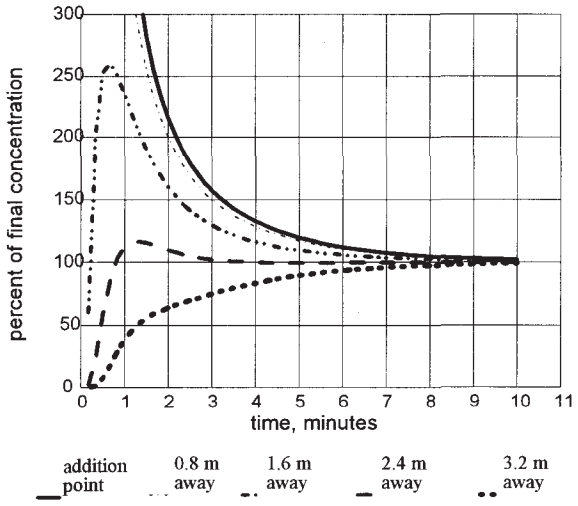

Figure 10: Predicted mixing rates along centre channel

Addition of alumina in the centre of the cell was simulated, and concentration transients at various locations in the centre channel were predicted, using the model with D_{eff} = 0.018 m^2s^{-1}. Mixing across the cell was not explicitly considered, as feeders are only installed in the centre channel.

Figure 10 shows the results of the simulation. The required concentration was reached 3.2 m from the addition point within one minute, and two feeders would be required for this cell, which is approximately 10 m in length.

4.4 Acceptable Concentration Gradients in Cell

To predict steady state concentration gradients set up in the cell, the cell was divided along its length into a number of perfectly-mixed tanks. The consumption of alumina in each tank, and the fluxes between tanks were determined, using the equation for steady state diffusion in one dimension. A worst-case scenario, in which only one feeder in the cell was operating near one end of the cell was considered (Figure 11(a)). This situation might occur if the cell had two feeders, one at each end, and one feeder was not operating. Variation in alumina concentration in the feed region over the feeding cycle were not modelled, and the concentration in the feeder tank was assumed constant at 3 %.

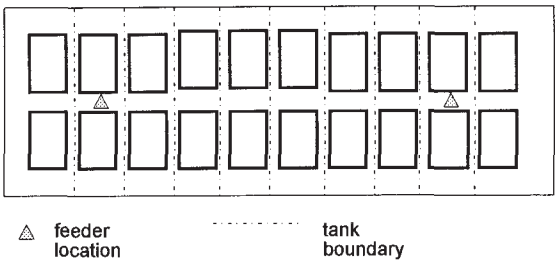

Figure 11(a): Division of cell into tanks

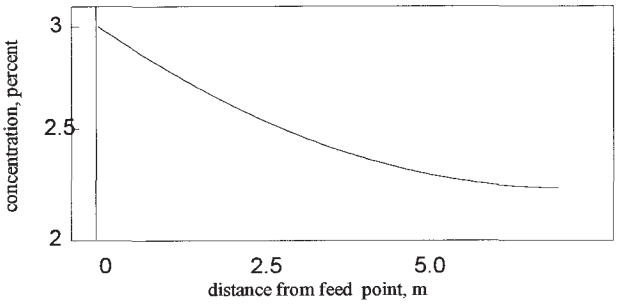

Figure 11(b): Predicted concentration gradients - one feeder

The concentration profile shown in Figure 11(b) predicts a concentration difference of 0.8 % between the two ends of the cell. Given that anode effects generally occur at 1.5 % or below[14,15], the cell should be operable even with only one feeder in this cell location. Except in a cell where mixing is particularly slow, preventing alumina concentration gradients is not expected to be the critical criterion for selecting the number of feeders in a cell.

5. CONCLUSIONS

Assuming that the water model and industrial tracer results presented in this paper accurately model alumina distribution in the cell, alumina dissolution occurs in a centre channel region the width of one or at most two anodes (depending on feeder location). Under the operating conditions considered, it has been estimated that an alumina addition of between 0.6 and 1.2 kg would cool the feed mixing zone to its liquidus temperature, for the cell geometry modelled. Slow dissolution of agglomerates and possibly sludge formation is expected to result if significantly larger masses of alumina are added.

The criteria proposed for avoiding alumina concentration gradients in the cell, and for rapid alumina distribution after an anode effect, are less stringent than those for good alumina dissolution, and are likely to be satisfied in cells designed according to current industry practice.

Results of laboratory investigations into continuous feeding of alumina show that, for alumina to dissolve immediately, extremely low addition rates are required. Based on these results and the estimated size of the mixing zone, and depending on feeder location, one continuous feeder would be required for every 25 to 50 kA of current. Further experimental work is required to determine under what conditions the floating alumina agglomerates formed at higher addition rates contribute to the formation of sludge.

REFERENCES

1. Liu, X., George, S.F., Wills, V.: 'Visualisation of Alumina Dissolution in Cryolitic Melts', TMS-AIME Light Metals 1994, pp. 359-364.

2. Rolseth, S., Hovland, R., Kobbeltvedt,O.: 'Alumina Agglomeration and Dissolution in Cryolitic Melts', TMS-AIME Light Metals 1994, pp. 351-357.

3. Liu, X., Purdie, J.M., Taylor, M.P. and Welch, B.J.: 'Measurements and Modelling of Alumina Mixing and Dissolution for Varying Electrolyte Heat and Mass Transfer Conditions', TMS-AIME Light Metals 1991, pp. 289-298.

4. Purdie, J.M., Bilek, M, Taylor, M.P., Zhang, W.D., Welch, B.J., Chen, J.J.J.: 'Impact of Anode Gas Evolution on Electrolyte Flow and Mixing in Aluminium Electrowinning Cells', TMS-AIME Light Metals 1993, pp. 355-360.

5. Kuschel, G.I.: 'The Effect of Alumina Properties and Smelter Operating Conditions on the Dissolution Behaviour of Alumina', PhD thesis, Auckland University, 1990.

6. Haverkamp, R.G.: 'Surface Studies and Dissolution Studies of Fluorinated Alumina', PhD thesis, Auckland University, 1992.

7. Phan-Xuan, D., Castanet, R., Laffitte, M., Gore, J.: 'Microcalorimetric Study of Alumina Dissolution on Cryolitic Baths', TMS-AIME Light Metals 1975, pp. 159-177.

8. JANAF Thermochemical Tables, Third Edition, published by the American Chemical Society and the American Institute of Physics.

9. Kachanovskaya, I.S., Siraev, S., Kurokhtin, A.N., Lebedeva, L.V., Zanin, S.A.: 'Electrolyte Circulation in an Aluminium Electrolytic Cell', Tsvetnye Metally, 1972(8), pp. 28-31.

10. Nikitin, A.V., Kryokovski, V.A., Mikhalitsin, N.S., Tsvetnye Metally, 16(8), 1975, pp. 37-40.

11. Jain, R.K., Tricklebank, S.B., Welch, B.J.: 'Interaction of Aluminas with Aluminium Smelting Electrolytes', TMS-AIME Light Metals, 1983, pp. 609-622.

12. Bagshaw, A.N., Kuschel, G.I., Taylor, M.P., Tricklebank, S.B., Welch, B.J.: 'Effect of Operating Conditions on the Dissolution of Primary and Secondary (Reacted) Alumina Powder in Electrolytes', TMS-AIME Light Metals, 1985, pp. 649-659.

13. Rolseth, S., Thonstad, J.: 'Agglomeration and Dissolution of Alumina in Cryolite Baths', Extraction, Refining and Fabrication of Light Metals, Proc. Intl. Symp., Ed. M. Sahoo and P. Pinfold, Canadian Industrial Metallurgy Vol 24, Ottawa, Ontario, 1991.

14. 'Introduction to Aluminium Electrolysis', Grjotheim, K. and Kvande, H. (editors), Aluminium Verlag, Dusseldorf, 1993, p. 210.

15. Thonstad, J.: 'Cell Voltage and Anode Effect' in 'The International course on Process Metallurgy of Aluminium', Trondheim, 1993.